C. R. Physique 11 (2010) 30–36

Contents lists available at ScienceDirect

Comptes Rendus Physique

www.sciencedirect.com

Propagation and remote sensing / Propagation et télédétection

Coupled reverberation chambers for emulating MIMO channels

Emulation de canaux MIMO grâce à des chambres réverbérantes couplées

Olivier Delangre [a,b], Philippe De Doncker [a], Martine Lienard [b,*], Pierre Degauque [b]

[a] *Université Libre de Bruxelles, Dept. OPERA, CP 194/5, 50, avenue F.D. Roosevelt, B-1050 Bruxelles, Belgium*
[b] *Université de Lille, IEMN/TELICE, Bldg P3, 59655 Villeneuve d'Ascq cedex, France*

ARTICLE INFO

Article history:
Available online 25 February 2010

Keywords:
Reverberation chamber
MIMO channel
Channel emulation
MSRC

Mots-clés :
Chambre réverbérante
Canal MIMO
Émulation de canaux
CRBM

ABSTRACT

This article describes a new experimental set up for emulating MIMO channels, based on two mode stirred reverberation chambers (MSRC), coupled together with a waveguide. This guide allows one to control the order of the channel diversity, the chambers generating a Rayleigh environment. This set up could thus be used to perform tests of MIMO communication systems in perfectly defined environments and thus under reproducible conditions. After a brief recall of the advantages and drawbacks of using a single reverberation chamber, we describe the theoretical approach and the experimental results for the analysis of two coupled chambers.

RÉSUMÉ

Cette contribution décrit un nouveau moyen d'émuler expérimentalement des canaux MIMO grâce à deux chambres réverbérantes à brassage de modes (CRBM), couplées entre elles par un guide d'onde. Ce guide permet de contrôler le degré de diversité du canal, les chambres générant des environnements de Rayleigh. Ce dispositif devrait permettre de tester expérimentalement les systèmes de communication MIMO dans des environnements parfaitement définis et donc reproductibles. Après avoir rappelé rapidement les potentialités et les limitations inhérentes à l'utilisation d'une chambre unique, nous décrirons l'approche théorique et les résultats expérimentaux qui ont été obtenus lors de l'analyse de deux chambres couplées.

1. Introduction

Reverberation chambers (RC) appear to be an interesting way to test communication systems using one transmitting and one receiving antenna. Each successive position of the stirrer corresponds to a realization of the channel. If the room is sufficiently oversized in terms of wavelength, thus assuming that it works in its normal operating range, the amplitudes of the transfer function between two antennas for different positions of the stirrer are distributed according to a Rayleigh distribution, provided that the consecutive positions of the stirrers are independent [1]. A Rice channel can also be emulated by optimizing the radiation pattern and the relative orientation of the transmitting and receiving antennas [2].

* Corresponding author.
E-mail address: Martine.Lienard@univ-lille1.fr (M. Lienard).

1631-0705/$ – see front matter
doi:10.1016/j.crhy.2009.11.002

However, there are restrictions involved in using an RC to emulate different types of propagation channels. First, the reflection coefficient on the large walls provokes a large spread of the impulse response. This difficulty can be avoided by introducing absorbers in the room to decrease the quality factor, thus reducing the delay spread. Another limitation is due to the isotropic nature of the angular spectrum at any point inside the chamber, which does not necessarily correspond to a real propagation environment, such as an urban or confined scenario. Various solutions have been proposed, but their implementations are quite cumbersome. As it stands, the RC lends itself well to the simulation of either a Rayleigh channel with uniformly distributed paths or a Rice channel.

Using an RC to simulate a MIMO (Multiple Input, Multiple Output) channel implies dealing with additional difficulties. Briefly, a MIMO channel can be considered to be composed of three zones: two are related to the nearby environment around the transmitting and receiving antenna arrays respectively, with the third one being related to the propagation between the two previous zones. For example, in certain situations, the propagation between the transmitter Tx and the receiver Rx can lead to a decrease in the rank of the channel matrix $\boldsymbol{H}$. In this case, $\boldsymbol{H}$ becomes a degenerated matrix, which also leads to a decrease in the channel capacity (in bit/s/Hz). This phenomenon is often called the "Keyhole" effect [3,4]. If the two transmitting and receiving arrays are placed in the same RC, it is impossible to change the characteristics of the propagation between them. For this reason, we propose using two RC coupled together by a waveguide [5]. Depending on the size of the guide, the number of non-evanescent modes for a given frequency is different, and the degree of channel diversity can thus be controlled.

In Section 2, the main characteristics of an RC are summarized, keeping in mind that the RC will be used as a means of testing performance of communication systems in Rayleigh environment. In Section 3, the results of some experiments that clearly show the interest of the coupled RC for emulating MIMO channels with various degrees of freedom, are reported. Section 4 is first devoted to a presentation of a theoretical model to predict the MIMO capacity in this environment. Then, the theoretical results are compared with those deduced from the measurements.

2. Main characteristics of a reverberation chamber for emulating a Rayleigh channel

Reverberation chambers have been used for many years in electromagnetic compatibility testing to evaluate the susceptibility of electronic devices illuminated by a uniform plane wave spectrum. RC have recently attracted the attention of the telecommunication industry since a plane wave spectrum is also found in traditional propagation channels (e.g., inside buildings or in confined environments). The first studies inside RC dealt with the characterization of handheld devices, such as cell-phones, but some studies have also examined the behavior of multi-antenna systems [6].

In order to be able to use RC to emulate real propagation channels, it is necessary to first find the link between the usual RC metrics (e.g., quality factor Q, energy decay factor τ_{RC}, mode bandwidth B_m) and the traditional propagation parameters (e.g., delay spread S_τ and coherence bandwidth B_c). It has been shown analytically [7] that, for a large quality factor, S_τ is given by the same expression as τ_{RC} and thus is easily related to the quality factor Q and to the carrier frequency f_c by:

$$S_\tau = \frac{Q}{2\pi f_c} \tag{1}$$

Similarly, the coherence bandwidth B_c, calculated for an amplitude of the complex correlation coefficient of the propagation channel $H(f)$ equal to 0.7, is given by:

$$B_c = \frac{f_c}{Q} \tag{2}$$

For a classic chamber, Q will have a very high value, ranging from 10 000 to 50 000, leading to very long propagation delays (i.e., up to 1 μs). These delays are much higher than what has been observed inside buildings. Simply putting absorbers inside the RC makes it possible to lower this delay spread easily.

To validate this approach, measurements were carried out in 3 different RC with volumes of 65 m^3, 16 m^3 and 9 m^3, respectively called in the rest of this text: large, medium and small RC. Various numbers of absorbers, each one having a surface of 1.4 m^2, were placed in each of these RC. Fig. 1 presents the measurement results, showing the delay spread for the 3 different RC as a function of the Q factor. The different delay spreads and Q factors were obtained by changing the number of absorbers.

During this measurement campaign, the transfer function between the antennas was measured with a vector network analyzer in a frequency bandwidth of 200 MHz around the center frequency of 5 GHz. From this frequency analysis, the impulse response was obtained by using a Fourier transform, allowing the delay spread to be computed. The quality factor was deduced from the well-known formula, relating the received and transmitted power, P_r and P_t [2]:

$$Q = \frac{16\pi^2 V}{\lambda^2} \frac{\langle P_r \rangle}{P_t} \tag{3}$$

where V and λ are respectively the volume of the RC and the wavelength.

For example, the quality factor was reduced to 2500 when placing 4 absorbers in the large RC, leading to a delay spread of 80 ns, which is quite similar to the value obtained in an indoor environment. The continuous line in Fig. 1 was plotted

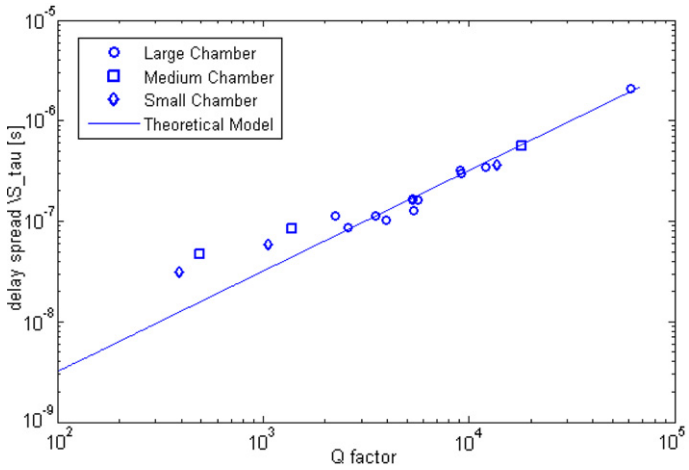

Fig. 1. Delay spread and quality factor of various chambers depending on the number of absorbers.

Fig. 1. Étalement des retards et coefficient de qualité de diverses chambres pour un nombre divers de panneaux absorbants.

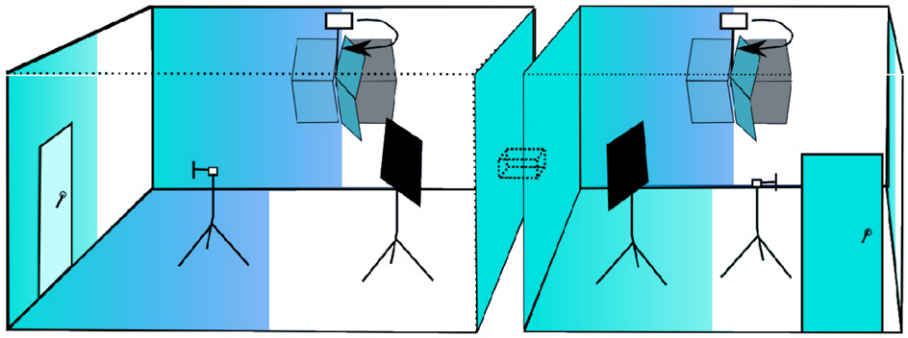

Fig. 2. Chambers coupled together with a waveguide.

Fig. 2. Chambres couplées par un guide d'onde.

by applying the theoretical relationship between S_τ and Q given by (1). As can be seen in this figure, this theoretical line matches the curve deduced from measurements quite well, as long as the Q factor is sufficiently high, above 2500 in this case. It is thus possible to emulate Rayleigh channels with delay spreads between 80 ns and 1 µs, which is a large enough range to simulate a wide range of realistic environments from indoor to outdoor. However, in an RC the angular spectra of the waves are uniformly distributed and thus cannot be easily used to emulate clusters.

When using RC to test the performance of a MIMO communication system, the rank of the channel is of great importance. The maximum rank is equal to the minimum number of antenna elements at the Tx and Rx sites. In the rest of this article, we consider that the Tx and Rx arrays have the same number of elements. In the cases of degenerated channels, the rank is lower, leading to poorer performances. To emulate such channels, degenerated or not, we propose an experimental setup based on two reverberation chambers.

3. Using coupled reverberation chambers to emulate MIMO channels: an experimental approach

3.1. Set up and experimental results

In order to control the diversity degree of a propagation channel, corresponding to the rank of the $\boldsymbol{H}$ matrix, we propose a new set up composed of two reverberation chambers connected together with a waveguide whose transverse dimensions can be changed. The set up is illustrated in Fig. 2.

Each antenna array is placed in a different RC. By choosing waveguides with different transverse dimensions, the number of propagating modes can be controlled, thus also controlling the degree of channel diversity. The rank of the channel is directly related to the amplitude of the singular values of the channel matrix $\boldsymbol{H}$. The channel matrix is thus fully degenerated (i.e., only one degree of freedom) if the transmitting signal's carrier frequency is smaller than the cut-off frequency of the second waveguide mode f_{c2}.

Let us consider a waveguide with transverse dimensions of 7.1×2.2 cm and a frequency bandwidth extending from 3.8 to 4.5 GHz. For this configuration, the second mode's cut-off frequency TE_{20} is 4.22 GHz. Using a vector network analyzer,

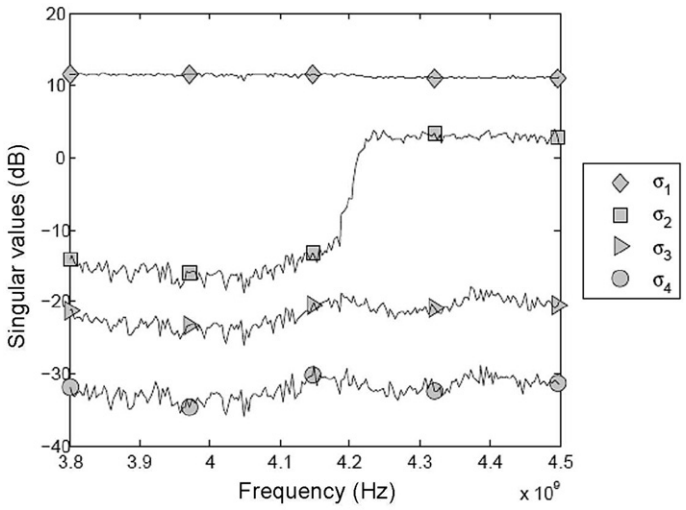

Fig. 3. Singular values versus frequency for a 4×4 MIMO link.

Fig. 3. Valeurs singulières en fonction de la fréquence pour une liaison MIMO 4×4.

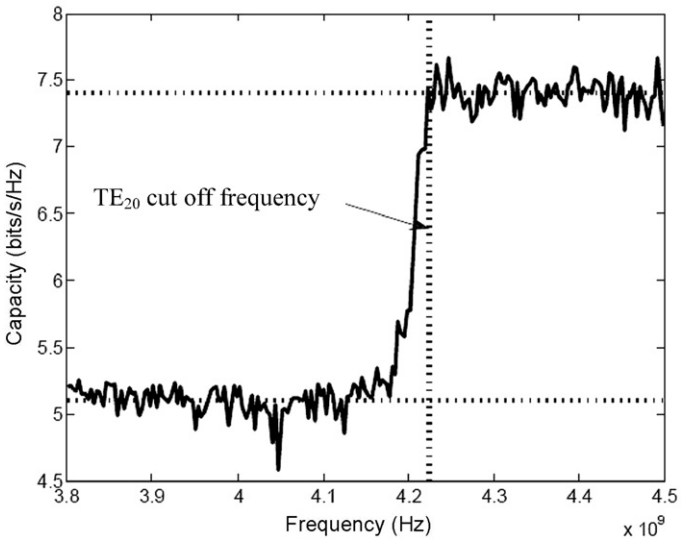

Fig. 4. Capacity of a 4×4 MIMO channel versus frequency.

Fig. 4. Variation de la capacité du canal MIMO (4×4) en fonction de la fréquence.

the transfer matrix was measured between the two antenna arrays. To simulate a MIMO link, we used the concept of virtual arrays, considering successive positions of the antennas. The measurements were made under static conditions, i.e. when both the stirrer and the antennas were not moving. The overall system was monitored, using optical fibers to avoid any interference. The singular values σ deduced from the measured $\boldsymbol{H}$ matrices are shown in Fig. 3.

Clearly, in Fig. 3, there is only one significant singular value below 4.22 GHz and two above. The ergodic capacity was calculated with the classic formula [8,9] below:

$$C = E_H\left\{\log_2\left[\det\left(I_M + \frac{SNR}{M} H H^{+}\right)\right]\right\} \tag{4}$$

where I is the identity matrix, M is the number of antennas (assumed to be the same for Tx and Rx), and $^{+}$ is the hermitian operator. The expectation is made for all channel realizations (i.e., over all positions of the stirrer).

The variation of the capacity of the 4×4 MIMO system versus frequency is shown in Fig. 4, assuming a signal-to-noise ratio *SNR* of 10 dB. The increase of the ergodic capacity can be observed at frequencies above 4.22 GHz, emphasizing the change in the degree of freedom of the channel.

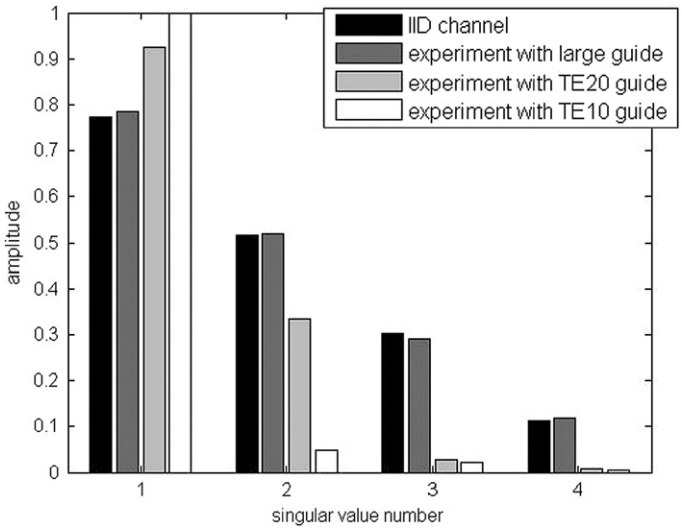

Fig. 5. Distribution of the singular values for various sizes of waveguide.

Fig. 5. Distribution des valeurs singulières pour différents types de guide.

Other measurements were taken at 3 GHz with waveguides with different transverse dimensions. The first guide was oversized, and thus able to support a large number of propagating modes at this frequency. The two others, called TE01 guide and TE02 guide, are able to support 1 mode and 2 modes, respectively. Fig. 5 shows the distribution of the singular values, deduced from a large number of channel realizations. Fig. 5 also presents the theoretical values obtained under the assumption of a perfectly iid (independently and identically distributed) channel, which are in quite good agreement with those obtained with the oversized waveguide. When the waveguide only supports 1 or 2 modes, only 1 or 2 singular values are significant, as seen in Fig. 5.

4. Modeling the MIMO channel emulated with coupled reverberation chambers

In order to obtain a full theoretical model, we first look at the excitation of the modes inside the waveguide. Then, we compare the experimental and theoretical amplitude distributions of the transfer matrix's eigenvalues, deduced with our channel model, based on a Kronecker approach.

4.1. Coupling between chambers

In order to compute the amplitude of the excited modes, let us first consider the electric field at any point $\vec{r}$ for a given time t (i.e., for a given position of the stirrer). This electric field is expressed as a sum of plane waves weighted by the incoming wave spectrum:

$$\vec{E}(t,\vec{r}) = \int_{\Omega} \vec{F}(t,\Omega) e^{-j\vec{k}.\vec{r}}\,\mathrm{d}\Omega \tag{5}$$

where $\vec{k}$ is the wave vector. The first assumption is that the incident spectrum on the waveguide of transverse surface S is isotropic on the half sphere Ω.

By computing the scalar product between the modal functions of the waveguide $\vec{e}_{nm}$ [10], associated to modes (n,m), and the incident electric field given by (5), the amplitude of each mode A_{nm} in the waveguide's entrance plane is obtained:

$$A_{nm} = \int_{S}\int_{\Omega} \vec{e}^{\,*}_{nm}(r)\vec{F}(t,\Omega) e^{-j\vec{k}.\vec{r}}\,\mathrm{d}S\,\mathrm{d}\Omega \tag{6}$$

However, (6) cannot be solved since the incident spectrum at any time t, is unknown. We chose a statistical approach for determining the properties of the RC. First, it is necessary to determine $\langle |A_{nm}|^2 \rangle$, the averaging being made over numerous positions of the stirrer. Then, by calculating the mean product of two amplitudes, A_{nm} and A_{pq}, and using (6), one obtains, in spherical coordinates [11]:

$$\langle A_{nm}, A^*_{pq} \rangle = \left\{ \int_{S}\int_{\Omega} \left[e^*_{\theta nm}(\vec{r}) F_\theta(t,\Omega) + e^*_{\phi nm}(\vec{r}) F_\phi(t,\Omega) \right] e^{-j\vec{k}.\vec{r}}\,\mathrm{d}S\,\mathrm{d}\Omega \right\}$$

$$\cdot\left\{\int_S\int_\Omega \left[e_{\theta pq}(\vec{r})F^*_\theta(t,\Omega)+e_{\phi pq}(\vec{r})F^*_\phi(t,\Omega)\right]e^{-j\vec{k}.\vec{r}}\,\mathrm{d}S\,\mathrm{d}\Omega\right\} \tag{7}$$

Since the θ and ϕ components of the incident spectrum are not correlated, the expression of the mean product of the incident spectrum given in [12] can be used. Consequently, (6) can be re-written as:

$$\langle A_{nm}, A^*_{pq}\rangle = \frac{E_0^2}{8\pi}\int_\Omega\left\{\int_S \vec{e}_{Tnm}(\vec{r})e^{-j\vec{k}\vec{r}}\,\mathrm{d}S\right\}\left\{\int_{S_2}\vec{e}_{Tpq}(\vec{r})e^{-j\vec{k}\vec{r}}\,\mathrm{d}S\right\}^*\mathrm{d}\Omega \tag{8}$$

where E_0^2 is the mean-square value of the electric field in the RC and $\vec{e}_{Tnm}$ is the transverse modal vector given by:

$$\vec{e}_{Tnm} = e_{\theta nm}\hat{\theta} + e_{\phi nm}\hat{\phi} \tag{9}$$

$\hat{\theta}$ and $\hat{\phi}$ are the unit vectors in spherical coordinates. From (8), it is straightforward to obtain $\langle|A_{nm}|^2\rangle$ for any excited mode:

$$\langle|A_{nm}|^2\rangle = \frac{E_0^2}{8\pi}\int_\Omega \left|C_{nm}(\Omega)\right|^2\mathrm{d}\Omega \tag{10}$$

In (10) $|C_{nm}(\Omega)|^2$ is calculated from the following integral:

$$\left|C_{nm}(\Omega)\right|^2 = \left|\int_S \vec{e}_{Tnm}(\Omega,\vec{r})e^{-j\vec{k}.\vec{r}}\,\mathrm{d}S\right|^2 \tag{11}$$

4.2. Channel model and experimental validation

A Kronecker approach [13,14] was chosen for modeling the MIMO channel. In this case, it was easy to start from the available equations and to extend them to our case. The transfer matrix is expressed as:

$$H = R_{RX}^{1/2}G_1 T G_2\left(R_{TX}^{1/2}\right)^T \tag{12}$$

In (12), R_{RX} and R_{TX} are the correlation matrices between antennas either at Rx or at Tx, and these matrices are deduced from an experimental or a theoretical approach [15]. The matrices G_1 and G_2 characterize the channel in each RC for a given position of the stirrer, and $\boldsymbol{T}$ is the transfer matrix of the waveguide. The matrix $\boldsymbol{T}$ is diagonal, since the modes in the waveguide are orthogonal. However, it is not possible to analytically relate a position of the stirrer to the wave spectrum in the waveguide's entrance plane. Nonetheless, if we consider a statistical approach, it is well known that the elements of G_1 and G_2 are Rayleigh distributed. Furthermore, the mean value of each diagonal term of $\boldsymbol{T}$ is given by:

$$T_{ii} = \sqrt{\langle|A_{n_i m_i}|^2\rangle}\exp\left(-(\alpha_i + j\beta_i)d\right) \tag{13}$$

In (13), $A_{n_i m_i}$ is the amplitude of the ith mode, TE_{nm} or TM_{nm}, among the N modes propagating inside the waveguide of length d. The terms α_i and β_i are the attenuation constant and phase constant in the guide.

In order to validate this theoretical approach, let us consider a frequency of 4.5 GHz, with the two RC being connected with a waveguide supporting two modes at this frequency. The spacing between the simulated MIMO array elements is 1.18λ. The cumulative probability density function of the two significant eigenvalues is shown by the continuous line in Fig. 6. The dashed line in the same figure represents the theoretical curve, which was obtained after randomly generating 1000 matrices, according to (12).

The cumulative distribution of the channel capacity, assuming a SNR of 10 dB, is represented in Fig. 7. This distribution was calculated from the $\boldsymbol{H}$ matrices, deduced either from the model or from our experiments.

Again, it is clear from Figs. 6 and 7 that there is a good match between the experimental results and the theoretical values obtained with the Kronecker model. This model has also been extended to include a wideband approach for determining the impulse response of these coupled chambers and for deducing its power delay profile [16].

5. Conclusion

We have shown that, using two reverberation chambers coupled with a waveguide, it is possible to emulate MIMO channels while controlling the degree of channel diversity. Indeed, the diversity is directly related to the number of non-evanescent modes propagating in the guide and thus on the transverse dimensions of the guide. For an oversized waveguide, the large number of modes leads to a full rank transfer matrix. Another advantage of this approach is that the propagation characteristics can be controlled separately around the transmitter and the receiver since the quality factor of each chamber can be modified by using different numbers of absorbers. With such a set up, it would be possible to test communication systems for various scenarios in a well-defined and reproducible environment.

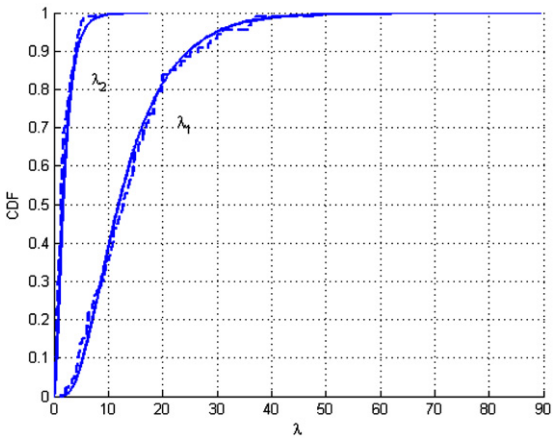

Fig. 6. Cumulative probability density function of the two eigenvalues, deduced either from measurements (dotted line) or from the model (continuous line).

Fig. 6. Densité cumulative de probabilité des deux valeurs propres, déduite soit des mesures (courbe en pointillé), soit du modèle (courbe en trait plein).

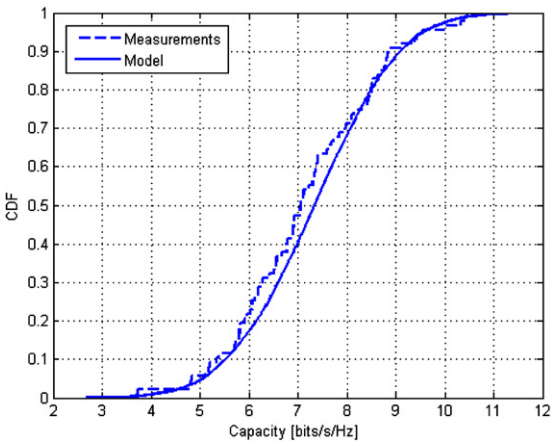

Fig. 7. Cumulative distribution function of the channel capacity. Comparison between predicted values based either on the measurement of ***H*** or on the Kronecker model.

Fig. 7. Densité de probabilité cumulée pour la capacité du canal entre les chambres. Comparaison entre les prévisions issues des mesures de ***H*** et celles du modèle de Kronecker.

Acknowledgement

This work was carried out within the frame of CISIT (International Campus on Safety and Intermodality in Transportation) and with the support of the FEDER funds, the French Ministry of research and the Region Nord Pas-de-Calais (France).

References

[1] O. Delangre, et al., Analytical angular correlation function in a mode-stirred reverberation chamber, Electron. Lett. 45 (2009) 90–91.
[2] C.L. Holloway, et al., On the use of reverberation chambers to simulate a Rician radio environment for the testing of wireless devices, IEEE Trans. Antennas and Propagation 54 (2006) 3167–3177.
[3] D. Chizhik, et al., Capacities of multi-element transmit and receive antennas: correlations and keyholes, Electron. Lett. 36 (2000) 1099–1100.
[4] P. Almers, F. Tufvesson, A. Molish, Keyhole effect in MIMO wireless channels: Measurements and theory, IEEE Trans. Wireless Comm. 5 (2006) 3596–3604.
[5] M. Lienard, P. Degauque, Simulation of dual array multipath channels using mode stirred reverberation chamber, Electron. Lett. 40 (2004) 578–580.
[6] K. Rosengren, P. Kildal, Radiation efficiency, correlation, diversity gain and capacity of a six-monopole antenna array for a MIMO system: Theory, simulation and measurement in a reverberation chamber, IET Proc. Microwaves, Antennas and Propagation 152 (2005) 7–16.
[7] O. Delangre, et al., Delay spread and coherence bandwidth in reverberation chamber, Electron. Lett. 44 (2008) 328–329.
[8] G.J. Foschini, M.J. Gans, On limits of wireless communications in a fading environment when using multiple antennas, Wireless Personal Comm. 6 (1998) 311–335.
[9] I.E. Telatar, Capacity on multi-antenna Gaussian channel, European Trans. on Telecom. 10 (1995) 585–595.
[10] R.E. Collin, Field Theory of Guided Waves, McGraw–Hill, New York, 1960.
[11] P. De Doncker, R. Meys, Statistical response of antennas under uncorrelated plane wave spectrum, Electromagnetics 24 (2004) 409–424.
[12] O. Delangre, Caractérisation et modélisation du canal radio en chambre réverbérante, Thèse Doctorat Univ. Lille et Univ. Libre de Bruxelles, 2008.
[13] D. Chizhik, et al., Effect of antenna separation on the capacity of BLAST in correlated channels, IEEE Comm. Lett. 4 (2000) 337–339.
[14] D. Gesbert, et al., MIMO wireless channels: capacity and performance prediction, IEEE Proc. Globecom 2 (2000) 1083–1088.
[15] O. Delangre, et al., Effect of 3D antenna parameters on MIMO systems with experimental validation, in: IEEE Symposium on Vehicular Technology in the Benelux, Ghent, Belgium, 2004.
[16] O. Delangre, et al., Wideband analysis of coupled reverberation chambers for testing MIMO systems, in: IEEE PIMRC Conf., 2006.